Climate Dynamics (2018) 51:3009–3021
https://doi.org/10.1007/s00382-017-4061-7

Enhancement of the spring East China precipitation response to tropical sea surface temperature variability

Mengqi Zhang[1,3] · **Jianqi Sun**[1,2,3]

Received: 1 September 2017 / Accepted: 16 December 2017 / Published online: 26 December 2017

Abstract
The boreal spring relationship between variabilities of East China precipitation (ECP) and tropical Ocean sea surface temperature (SST) during the period 1951–2014 is investigated in this study. The results show that the leading mode of the ECP variability exhibits an enhanced response to the anomalous El Niño–Southern Oscillation (ENSO)-like SST after the late 1970s, when the SST underwent a decadal change, with two positive centers over the eastern tropical Pacific (ETP) and tropical Indian Ocean (TIO). To further understand the relative roles of the ETP and TIO SST anomalies (SSTAs) in the variability of ECP after the late 1970s, partial regression and correlation methods are used. It is found that, without the contribution of the TIO, ETP SSTA plays a limited role in the variability of ECP after the late 1970s; comparatively, a significant correlation between TIO SST and ECP is identified during the same period, when the ETP signal is linearly removed. Physical analyses show that, after the late 1970s, the TIO SSTA affects East Asian atmospheric circulation in two ways: by exciting a zonal wave-train pattern over the mid-latitude Eurasian Continent and by inducing anomalous convection over the Maritime Continent. Via these two mechanisms, the TIO SST variability results in an anomalous East Asian trough and vertical motion over East China and consequently leads to anomalous precipitation over the region. The physical processes linking the ECP and TIO SST are confirmed by an atmospheric general circulation model experiment forced with idealized TIO warming.

Keywords East China spring precipitation · Tropical SST · ENSO · Interdecadal change

1 Introduction

In spring, anomalous precipitation is generally associated with droughts and floods, severely disrupting spring plowing and agricultural production. Therefore, understanding the variability of precipitation and its mechanism is of great socio-economic importance, particularly for eastern China, which has a population of nearly 1 billion.

Wang et al. (2002) defined the South China spring monsoon and found that the monsoon interannual variability is primarily related to circulation anomalies over the North Pacific, which is different from that during the East Asia summer or winter monsoon season. Zhang et al. (2009) revealed the spatial distributions of anomalous East China precipitation (ECP) in boreal spring and its related atmospheric circulations over the period 1951–1999: rainfall anomalies in South China are related to the intensification of the western Pacific subtropical high (WPSH) and southwestward East Asian jet stream (EAJS); rainfall anomalies in the middle and lower reaches of the Yangtze River valley are accompanied by a northward shift of the WPSH and EAJS; rainfall anomalies over the Huaihe River Valley correspond to a 500 hPa anticyclone anomaly near the Japan Sea and a weaker EAJS. Zhou and Zhao (2010) suggested a strong linkage between spring precipitation over central East China and the simultaneous Asian–Pacific Oscillation (APO). Xin et al. (2006) and Shao and Zhang (2012) showed a closed relationship between winter North Atlantic Oscillation (NAO) and following spring rainfall over East China during

✉ Jianqi Sun
sunjq@mail.iap.ac.cn

[1] Nansen-Zhu International Research Center, Institute of Atmospheric Physics, Chinese Academy of Sciences, P.O. Box 9804, Beijing 100029, China

[2] Collaborative Innovation Center on Forecast and Evaluation of Meteorological Disasters, Nanjing University of Information Science and Technology, Nanjing 210044, China

[3] University of Chinese Academy of Sciences, Beijing 100049, China

past half century. Zhou (2013) further suggested the impact of winter NAO on the spring precipitation over southern China weakened after the early 1980s. Li et al. (2016) suggested that the intensified convection over the South China Sea and the Philippine Sea is responsible for the declining trend of springtime rainfall over southern China.

In addition to the internal dynamics of atmospheric circulation, the tropical sea surface temperature (SST), which acts as an important external forcing, is also documented to be responsible for the variability of spring precipitation over East China. Zuo et al. (2012) observed that the variation in spring precipitation over mid-latitude East China is significantly correlated with the tropical Pacific SST in the preceding winter and the simultaneous spring during 1979–2004. Using recent 28-year observed data, Feng and Li (2011) demonstrated that the typical El Niño–Southern Oscillation (ENSO) and ENSO Modoki have opposite effects on South China spring precipitation: the typical ENSO event is accompanied by enhanced rainfall, whereas the ENSO Modoki is associated with reduced rainfall. A recent work documented that the relationship between spring precipitation over South China and ENSO is modulated by the Pacific Decadal Oscillation (PDO, Wu and Mao 2016). The relationship is enhanced when ENSO and PDO are in-phase, whereas it becomes ambiguous in the out-of-phase case.

In the late 1970s, an interdecadal shift of SST was observed over the tropical Oceans (e.g., Nitta and Yamada 1989; Lau and Weng 1999; Wu and Wang 2002; Guo and Yang 2002; Terray and Dominiak 2005). The Asian summer and winter climate associated with tropical SST underwent notable changes around the similar time, concurrently with the tropical Ocean SST interdecadal shift (e.g., Kumar et al. 1999; Gong and Ho 2002; Ding et al. 2010; Wang and He 2012). Thus, it is of particular interest to examine whether the relationship between spring tropical SST and ECP altered. If so, SSTAs over which tropical ocean region is critical in affecting the variability of ECP? This study was performed to address these questions. The paper is organized as follows: the datasets and model information are described in Sect. 2; the relationship between the spring ECP and tropical SST is investigated in Sect. 3; Sect. 4 examines the respective contributions of TIO and ETP SSTAs to the variability of ECP; Sect. 5 provides the results of numerical simulations; and conclusions are summarized in Sect. 6.

2 Datasets and model

The observed monthly precipitation data from 160 stations in China spanning the period 1951–2014 are obtained from the National Climate Center of the China Meteorological Administration. In this study, East China indicates the region east of 100°E. Based on this criterion, 140 stations are selected. The precipitation anomaly percentage is used to represent the variability of precipitation, which is defined as the percentage of precipitation anomaly relative to the climatology for each station. In this study, there are two climatological periods: one is 1951–2014 and the other is 1981–2014. An anomaly is departure from the climatological mean during the target period. In this study, spring is referred to as the mean of March–April–May.

The atmosphere circulation dataset used in this study is the monthly mean reanalysis derived from the National Centers for Environmental Prediction–National Center for Atmospheric Research (NCEP–NCAR), which has a resolution of 2.5° × 2.5° and covers the period from 1948 to the present (Kalnay et al. 1996). The analysis variables include geopotential height, horizontal wind and vertical velocity. The SST dataset is the National Oceanic and Atmospheric Administration (NOAA) extended reconstructed SST version 4 (ERSST.v4), which has a resolution of 2° × 2° and covers the period from 1854 to the present (Huang et al. 2015). The Niño3 index obtained from the NOAA Climate Prediction Center (CPC) over the period 1950–2015 is used to represent the variability of the ETP. All analyses of the data are confined to the common time period of 1951–2014.

We perform numerical simulations to further discuss the impact of TIO warming based on the Community Atmosphere Model (CAM4) (Gent et al. 2011). The CAM4 is the atmospheric component of the Community Earth System Model (CESM1_0_5). Two simulations are performed. In the control run (EXP0), the CAM4 is coupled with an active land model (Community Land Model), forced by the climatological SST and sea ice and run with a 1.9° × 2.5° finite volume grid, 26 hybrid sigma pressure levels, a 30-min integration time step, and a CO_2 concentration of 367.0 ppm. The sensitivity run (EXP1) is similar to EXP0 but with a homogeneous SST anomaly of 0.5 °C added over the TIO domain of (40°–110°E, 20°S–20°N). To avoid abrupt changes in SST, the TIO SST anomaly is linearly decreased to 0 °C at the four edges of the region. Twenty-five-year runs are performed. The first 5 years represent the model spin-up time, and the remaining 20 years are used for analysis.

3 Interdecadal change in the relationship between spring ECP and tropical SST

Figure 1 depicts the first leading empirical orthogonal function mode (EOF1) of the spring ECP variability for the period 1951–2014. The spring ECP generally exhibits consistent spatial variability with a peak value in North China, except for some small regions with weak opposite variability over the southern and northeastern parts of the region. The ECP EOF1 accounts for 23.8% of the

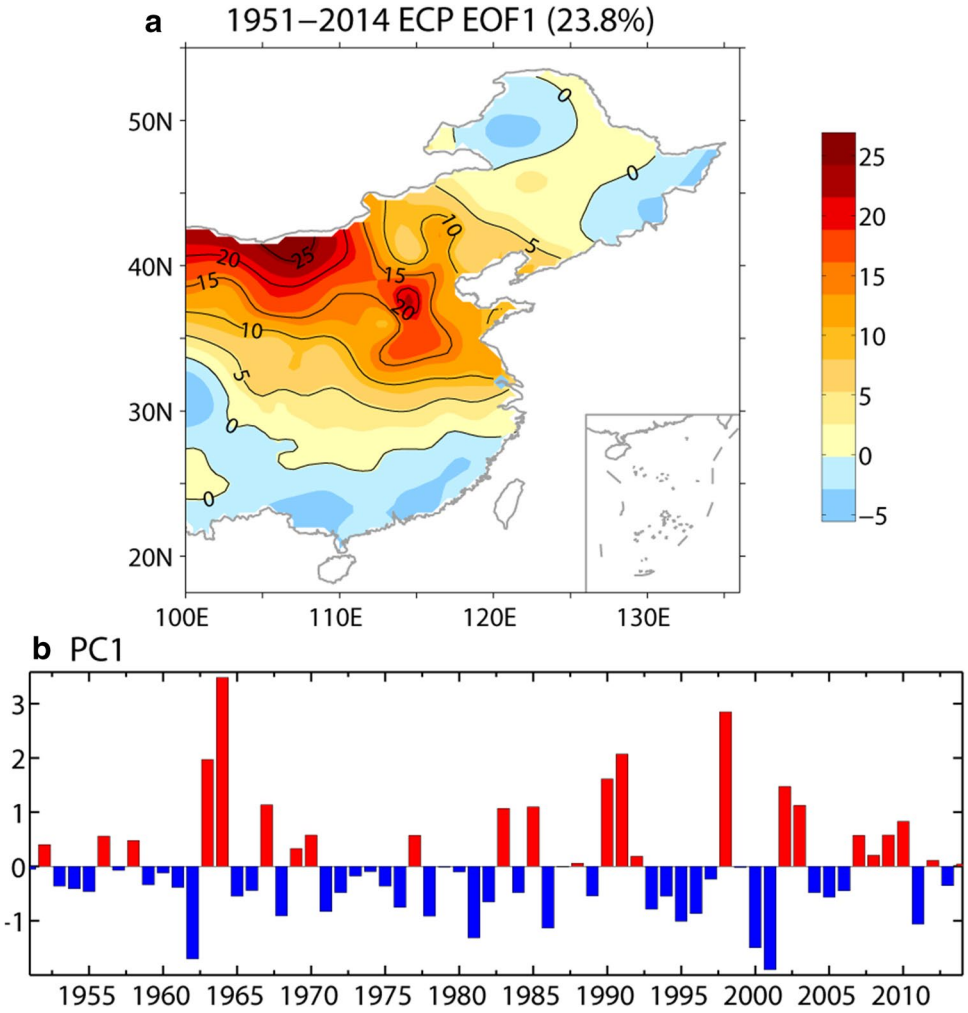

Fig. 1 **a** The first leading empirical orthogonal function mode (EOF1) of spring ECP during 1951–2014. **b** The corresponding normalized time series (PC1)

total variance. The time series of the EOF1 (PC1) exhibits strong year-to-year fluctuations.

A large number of studies have documented that the relationship between the East Asian climate and its external forcing factors experienced a notable shift around the late 1970s (e.g., Wang 2002; Wu and Wang 2002; Zhu et al. 2007; Sun et al. 2008; Sun 2012; Sun and Wang 2012; Zhou and Xia 2012). Therefore, the question naturally arises: is the link between the spring ECP and tropical SST stable over the past half century? To address this question, the correlation maps of SSTAs associated with the ECP PC1 in 1951–1975 and 1981–2014 are presented in Fig. 2. Before the late 1970s, there are few large-scale areas of significance over the tropics associated with a positive ECP anomaly. In contrast, after the late 1970s, there are significant positive SSTAs over the ETP and TIO and weak negative SSTAs over the tropical western Pacific, resembling an ENSO-like SST structure. These results suggest an enhanced relationship between the dominant mode of the spring ECP and tropical SST after the late 1970s.

Furthermore, the EOF1 of spring tropical SSTA over the region (40°E–80°W, 20°S–20°N) is examined for the period 1951–2014, as shown in Fig. 3a. The result suggests that the dominant pattern of tropical SSTA shows a consistent spatial distribution with the ECP PC1-related tropical SSTA during the period 1981–2014. Strong positive SSTAs are observed over the ETP and TIO, accompanied by relatively weak negative SSTA over the western tropical Pacific, mimicking an ENSO-like SST structure. Figure 3b shows the normalized SST PC1, which exhibits a distinct upward trend, implying persistent tropical SST warming during the past half century. The 9-year running means experience an abrupt change in sign from negative to positive around the late 1970s, which is significant at the 95% confidence level, according to a Student's *t* test.

Previous studies have suggested that the increased mean state and variation of tropical SST are responsible for the change in associated circulations and further alter the impact on climate variabilities (e.g., Huang et al. 2010; Xie et al. 2010; Qu and Huang 2012; Chen et al. 2014). Figure 4 depicts the 21-year running correlations between

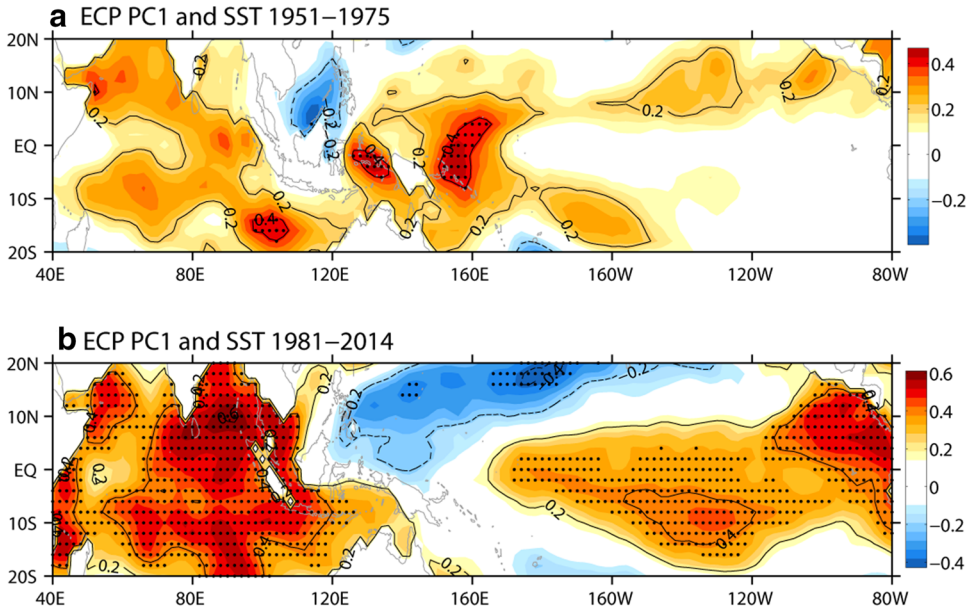

Fig. 2 The correlations of tropical SST associated with ECP PC1 in **a** 1951–1975 and **b** 1981–2014. Areas significant at the 95% confidence level are denoted by dots

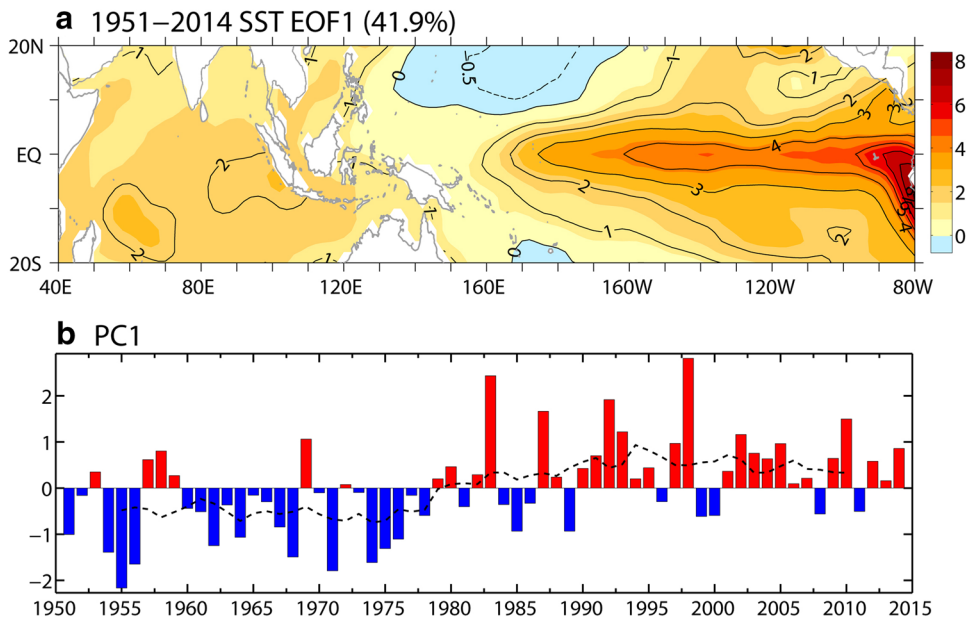

Fig. 3 Same as Fig. 1, but for SST over the region (40°E–80°W, 20°S–20°N). The dashed line in **b** depicts the 9-year running means

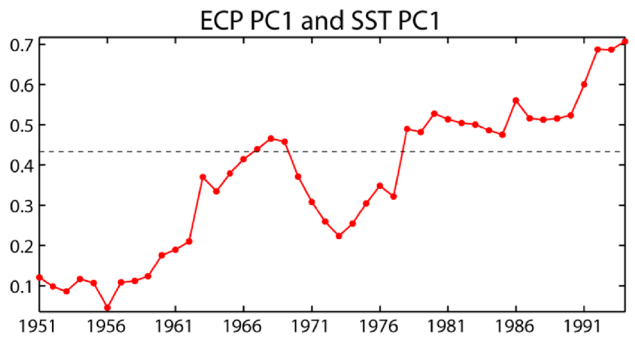

Fig. 4 The running correlations between ECP PC1 and SST PC1 for the period 1951–2014, presented at the first year of a 21-year window. The dashed line indicates the 95% confidence level

ECP PC1 and SST PC1 for the period 1951–2014. To avoid the possible effect of linear trends, all datasets have been detrended in the target period in the following analyses. The correlation coefficients depict an increasing trend, and they are stably significant over the period after the late 1970s. This result demonstrates an enhanced connection between the dominant variabilities of the spring ECP and tropical SST after the late 1970s, along with the decadal change in the tropical SST around the similar time.

To understand the unstable connection between the spring ECP and tropical SST over the past half-century, the two sub-periods of 1951–1975 (P1) and 1981–2014

(P2) are selected and the SST PC1-related large-scale atmospheric circulations are analyzed.

Figure 5a–d depict the simultaneous regression patterns of spring geopotential heights and horizontal winds at 850 and 500 hPa against the SST PC1 over the two sub-periods. Over the tropics, associated with a positive-phase ENSO-like tropical SST, a zonal-oriented dipole pattern is observed in the lower troposphere, with significant positive anomalies over the TIO and western tropical Pacific and negative anomalies over the ETP in both sub-periods (Fig. 5a, b). Over the central-eastern tropical Pacific, anomalous westerlies are closely related to the ENSO events (Fig. 5a, b). At the middle level, a consistent positive anomalous belt is found to dominate the tropics (Fig. 5c, d).

Notable differences in SST PC1-related circulations between the two sub-periods are observed over the middle latitudes. During P1, the spatial distribution of the anomalous geopotential heights at 500 hPa indicates a North Pacific Oscillation (NPO) and a Pacific-North American (PNA) pattern over the North Pacific region (Fig. 5c). Such mid-level anomalous circulation patterns are also reflected in the lower level as a deepened Aleutian Low and an anticyclonic anomaly over the western tropical Pacific (Fig. 5a). However, over East Asia, the geopotential height and wind anomalies are both quite weak, demonstrating a weak relationship between the tropical SST and East Asian atmospheric circulations during P1. In contrast, during P2, associated with the positive-phase ENSO-like tropical SSTA, the spatial distribution of the anomalous 500 hPa geopotential height over the middle latitudes indicates a West Pacific (WP) pattern and a PNA pattern over the North Pacific region (Fig. 5d). The WP pattern consists of a meridional dipole of anomalies with a negative center located over the Kamchatka Peninsula and a broad positive counterpart covering the region from southeastern Asia to the subtropical northwestern Pacific. The WP-related significant anomalous anticyclone indicates a weakened East

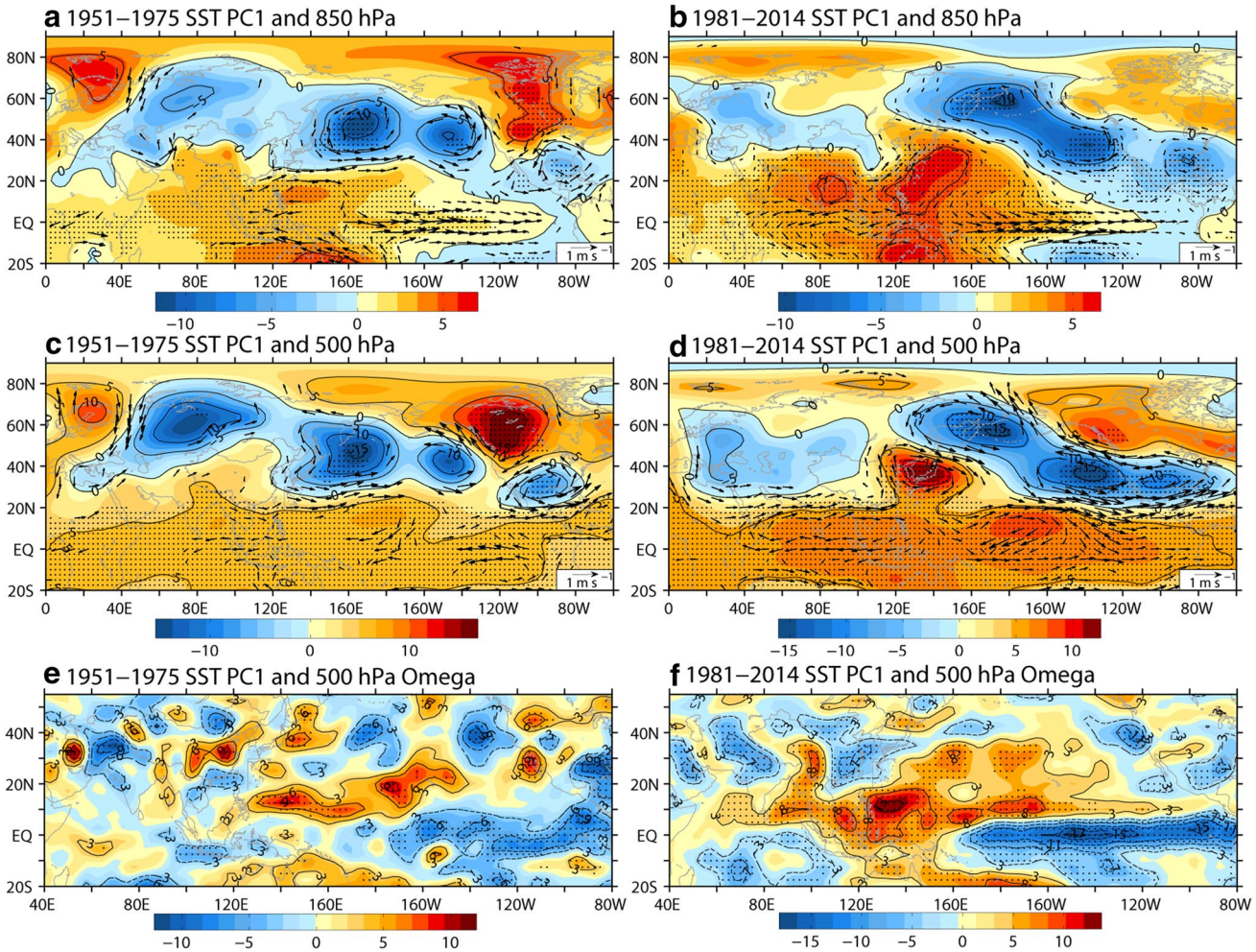

Fig. 5 Regressions of the geopotential height (colored shading in gpm) and horizontal wind (vectors in m s^{-1}) at **a, b** 850 hPa; **c, d** 500 hPa; and **e, f** 500 hPa omega (10^{-3} Pa s^{-1}) against SST PC1 for 1951–1975 (left panels) and 1981–2014 (right panels). Areas significant at the 95% confidence level are denoted by dots, and vectors at the 90% significant level are shown

Asian trough at the middle level, which is accompanied by strong anomalous anticyclones over the western North Pacific at the lower level. The weakened East Asian trough and strong western North Pacific anticyclone result in significant anomalous southerly wind over East Asia, favoring the northward intrusion of warm and wet air to East China and enhancing precipitation there.

Because the tropical convection is dependent on local SST, the anomalous vertical activity is further examined in the different tropical SST backgrounds. The vertical velocity anomaly covaries well with the convection variability in the tropics. Therefore, it is reasonable to use the 500 hPa vertical velocity (omega) to represent the convection activity over the region. Figure 5e, f depict the 500 hPa omega anomalies regressed upon the SST PC1 during the two sub-periods, which suggest that, along with the warming of SST over the tropics, the response of convection to the SST variability over the tropics is significantly enhanced after the late 1970s. During P1, significant tropical ascent motion is observed east of 170°W, with a peak value of -9×10^{-3} Pa s^{-1} near 90°W. The corresponding descent motion is observed over a limited region of the tropical western Pacific centered near 140°E, with a peak value of 9×10^{-3} Pa s^{-1}. In contrast, during P2, significant signals are expanded and intensified, dominating the tropical Pacific. The pronounced ascent motion over the central-eastern tropical Pacific is found to expand westward to 170°E, with an increased center at approximately 150°W, reaching -17×10^{-3} Pa s^{-1}. Over the western tropical Pacific, significant large-scale signals are observed covering the Maritime Continent, with the peak value increasing to 13×10^{-3} Pa s^{-1}, located near 130°E.

These results suggest an enhancement and westward migration of anomalous Walker circulation associated with SST PC1 after the late 1970s. In particular, vertical activities over East China reveal quite different features between the two sub-periods. During P1, there is no large-scale upward motion over East China. In contrast, during P2, significant upward activities are observed over most of the region, indicating a close connection between tropical SST and ECP.

The foregoing analyses suggest that, along with tropical SST warming, the ENSO-like tropical SSTA could enhance its impact on the circulations over East Asia. Therefore, tropical SST plays a more important role in the ECP variability after the late 1970s, through affecting the East Asian trough, a lower-level anticyclone over the western North Pacific, and vertical motion over East China.

4 Relative roles of the ETP and TIO SSTAs in the ECP variability after the late 1970s

The previous section demonstrated an enhanced relationship between the tropical SST and spring ECP after the late 1970s. In addition, the significant SSTAs associated with ECP could be observed over a wide area across the tropics during P2, with two centers over the ETP and TIO (Fig. 2b). Previous studies have revealed that SSTAs over the TIO and ETP can contribute to climate variabilities dependently (e.g., Klein et al. 1999; Alexander et al. 2002; Lau and Nath 2003; Liu and Alexander 2007) and independently (e.g., Li et al. 2013; Chen et al. 2015; Fletcher and Cassou 2015). Thus, we want to diagnose the relative roles of the ETP and TIO SSTs in the spring ECP variability after the late 1970s. To this end, two indices are employed to describe the variability over the TIO and ETP SSTs. A TIO index is used to represent the Indian Ocean basin-wide variability, which is defined as the averaged SST over the TIO region of (40°–110°E, 20°S–20°N). The Niño3 index is used to represent the variability of ETP SST. Furthermore, the correlation coefficient between the TIO and Niño3 index is calculated for the period 1951–2014, yielding a value of 0.54. This result indicates that the fraction of mutual explanation between the TIO and ETP SSTs is approximately 29%, and the two regions' SSTs also have independent variability. To identify the relative contribution of the TIO and ETP to the spring ECP variability after the late 1970s, partial regression and correlation are employed in the present study, and all the following analyses are applied to TIO-free (ETP-free) variables.

4.1 Relationship between ETP-related (TIO-free) SST and spring ECP

The ETP-related and TIO-free spring precipitation over East China in P2 is examined first using observational station precipitation. As shown in Fig. 6a, there is no large-scale area of significance over East China. This result suggests that, after excluding the effect of the TIO, the ETP plays a limited role in the ECP variability after the late 1970s.

The ETP-related (TIO-free) anomalous geopotential heights and horizontal winds at 850 and 500 hPa during P2 are presented in Fig. 7a, b. A zonal dipole structure at the lower level and a consistent positive belt at the middle level are observed over the tropic geopotential height, which is closely related to the ENSO variability. Over the middle latitudes, the WP and PNA patterns associated with the tropical SST PC1 after the late 1970s (Fig. 5d) are replaced by NPO and PNA teleconnections over the North

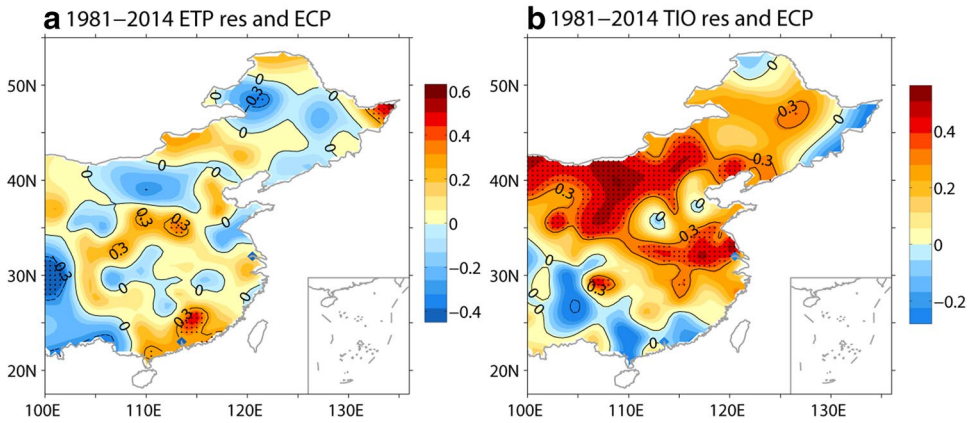

Fig. 6 The correlations of spring ECP associated with **a** ETP-related (TIO-free) SST (referred to as ETP res) and **b** TIO-related (ETP-free) SST (referred to as TIO res) for the period 1981–2014. Areas significant at the 95% confidence level are denoted by dots

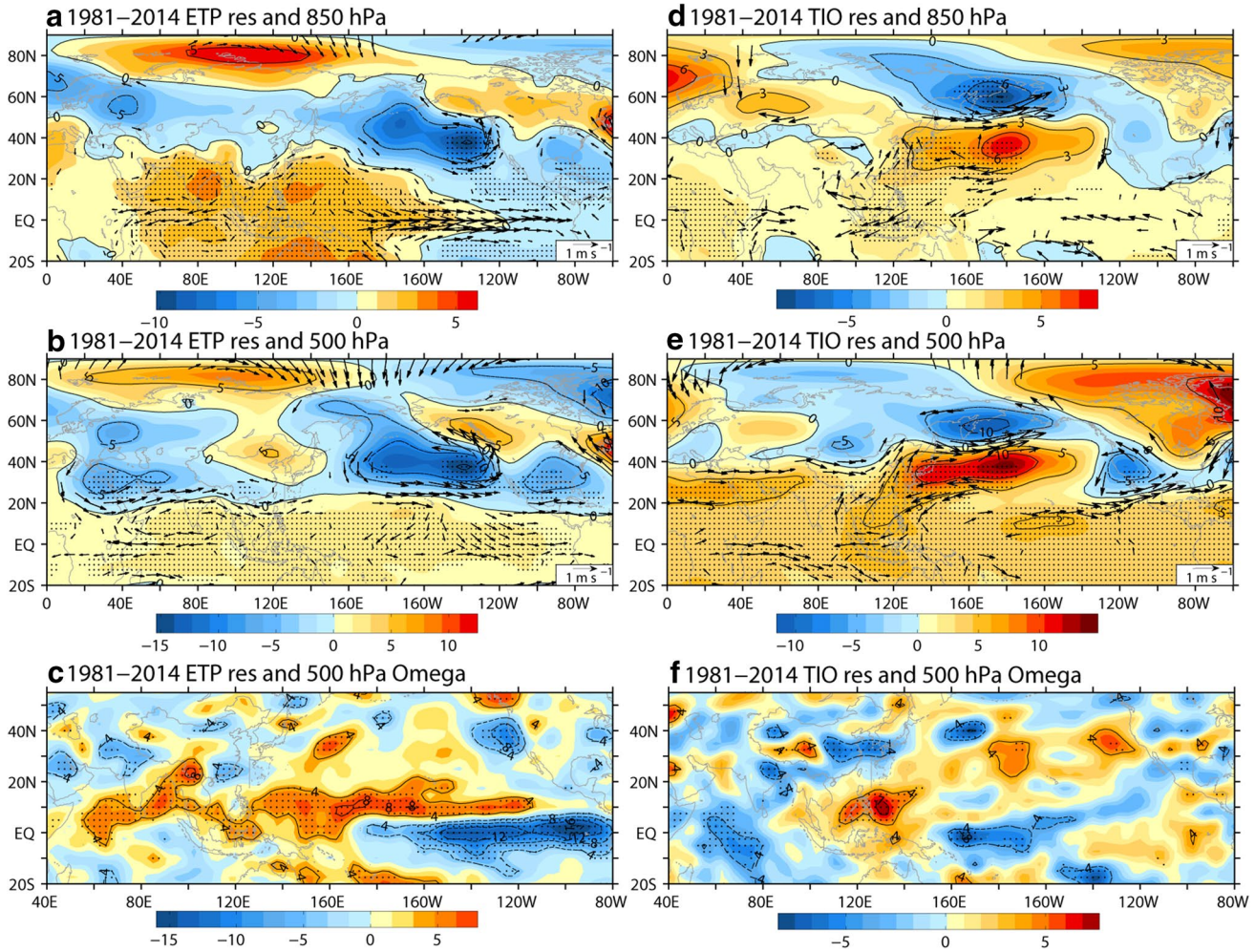

Fig. 7 Same as Fig. 5, but for ETP-related (TIO-free) SST (left panels; referred to as ETP res) and TIO-related (ETP-free) SST (right panels; referred to as TIO res) during the period 1981–2014. Areas significant at the 95% confidence level are denoted by dots, and vectors at the 90% significant level are shown

Pacific (Fig. 7b). Additionally, there is no large-scale significant signal over East Asia, indicating a weak impact of ETP-related (TIO-free) SST on ECP after the late 1970s.

Figure 7c depicts the ETP-related (TIO-free) vertical velocity, which has both common and distinct features with that associated with the tropical SST PC1 after the late 1970s

(Fig. 5f). A zonal dipole structure can still be observed over the tropical Pacific, with anomalous upward and downward motions over the eastern and western tropical Pacific, respectively; however, the spatial extent and intensity of the convection centers are notably different from those displayed in Fig. 5f. Pronounced upward activity is observed east of 170°W, with a peak value of -16×10^{-3} Pa s^{-1} centered near 100°W, which is weakened and clearly retreats eastward compared with that in the tropical EOF1 SST case. The corresponding downward activity still occurs over the western tropical Pacific; however, the large-scale significant signal over the Maritime Continent displayed in Fig. 5f is weakened here. In addition, the significant upward motions are confined over a small area across southern coastal China, confirming the weak connection between the independent ETP and spring ECP after the late 1970s.

4.2 Relationship between TIO-related (ETP-free) SST and spring ECP

Unlike the ETP-related (TIO-free) SST, the TIO-related (ETP-free) SST has a strong connection with the spring ECP (Fig. 6b). Significantly positive precipitation anomalies are observed over large areas of East China, sharing a highly similar spatial distribution with that associated with ECP EOF1 shown in Fig. 1a. The partial correlation coefficient between ECP PC1 and the TIO index in P2 is 0.47, significant at the 99% confidence level. These results demonstrate a close connection between TIO-related (ETP-free) SST and the dominant variability of ECP after the late 1970s.

The TIO-related (ETP-free) geopotential heights and horizontal winds at 850 and 500 hPa during P2 are displayed in Fig. 7d, e. A zonally positive belt is observed over the tropics in both the lower and middle troposphere. In addition, the anomalous westerlies and easterlies over the western and eastern parts of the TIO at 850 hPa indicate a strong low-level convergence over the region, which is closely related to a warmer-than-normal local SST over the region. Over the middle latitudes of the North Pacific region, a significant WP pattern can be observed at 500 hPa. The anomalous anticyclone is associated with the WP pattern covering the East Asia trough region, indicating a weakened East Asian trough at the middle level. Along with the weaker East Asian trough, there is a stronger anticyclone over the northwestern Pacific, and anomalous southwesterly winds along the west boundary of the anticyclone bring warm and humid air from the tropics to East China, consequently providing favorable conditions for precipitation there.

Additionally, a zonal wave-like pattern is observed over the mid-latitude Eurasian Continent at the middle level, along the East Asian jet, which also contributes to the anticyclonic anomaly over East Asia (Fig. 7e). The alternate cyclone and anticyclone teleconnection could be explained as a Rossby response to the anomalous TIO heating forcing, according to the Gill-type pattern (Gill 1980). An upper-level zonal teleconnection pattern over mid-latitude Eurasia is also identified in summer, which is a portion of the circumglobal teleconnection (CGT), closely related to the anomalous Indian summer monsoon (ISM, Wang et al. 2001; Wu and Wang 2002; Ding and Wang 2005; Yim et al. 2014). The enhanced ISM rainfall anomaly is capable of generating an upper-level anticyclone to its northwest over west-central Asia, which propagates along the mid-latitude westerly related waveguide, featuring a zonally oriented wave train (Yim et al. 2014). Because of the different backgrounds between spring and summer, the wave pattern over mid-latitude Eurasia in response to spring TIO warming exhibits distinct features.

Figure 7f depicts the vertical velocity with respect to TIO-related (ETP-free) SST during P2. Corresponding to a warmer-than-normal TIO SST, a zonal dipole structure is observed over the TIO-western tropical Pacific, with significant ascent and descent centers over the TIO and Maritime Continent, indicating an anomalous Indian Ocean Walker circulation, consistent with previous studies (Watanabe and Jin 2003; Annamalai et al. 2005). Over East China, pronounced upward activity is observed over a large portion of the region, which confirms the close relationship between the independent TIO and ECP after late 1970s. The variability of SST over TIO is closely related to meridional circulation (Zhou and Wang 2006). Furthermore, the TIO-related (ETP-free) local meridional circulation averaged along 110°–140°E shows significant descent and ascent motion near 10°N and 30°N, which suggest that the Maritime Continent convection serves as a bridge connecting the TIO and East China through vertical circulation (figure not shown). These results reveal that a positive anomaly of TIO SST could suppress the convection over the Maritime Continent by modulating a zonal circulation and further result in upward motion over East China through a meridional circulation.

The convection over Maritime Continent is an important factor affecting the East Asian atmosphere circulation (Sun et al. 2009; Zhou 2011). To further investigate the connection between the TIO SST variability and Maritime Continent convection, a Maritime Continent omega index is defined as the 500 hPa omega averaged over the region (110°–140°E, 5°–15°N). Figure 8 depicts the running correlations between the Maritime Continent omega index and the spring TIO index with a 21-year window, after excluding the signal of the ETP. The correlations display an upward trend and become stably significant at the 95% confidence level after the late 1970s, which indicates a close relationship between the TIO SSTA and convection activity over the Maritime Continent during this period.

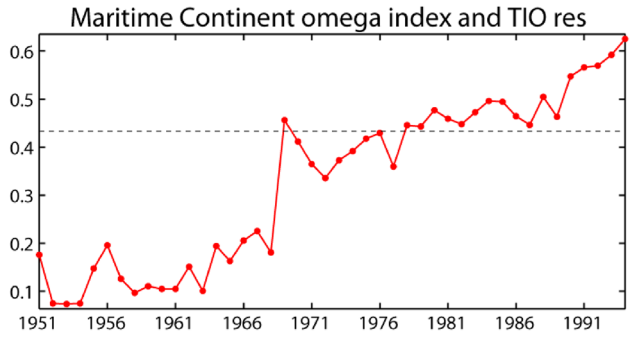

Fig. 8 The running partial correlations between the Maritime Continent omega index (ETP-free) and TIO index (ETP-free; referred to as TIO res) for 1951–2014, presented at the first year of a 21-year window. The dashed line indicates the 95% confidence level

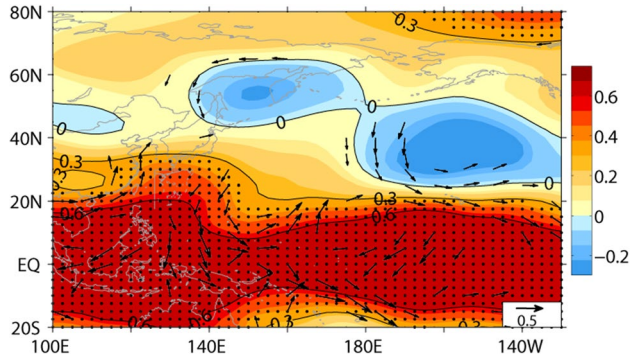

Fig. 9 Correlations of geopotential height (colored shading) and horizontal wind (vectors) at 500 hPa with respect to Maritime Continent omega index (ETP-free) for the period 1981–2014. Areas significant at the 95% confidence level are denoted by dots, and vectors at the 90% significant level are shown

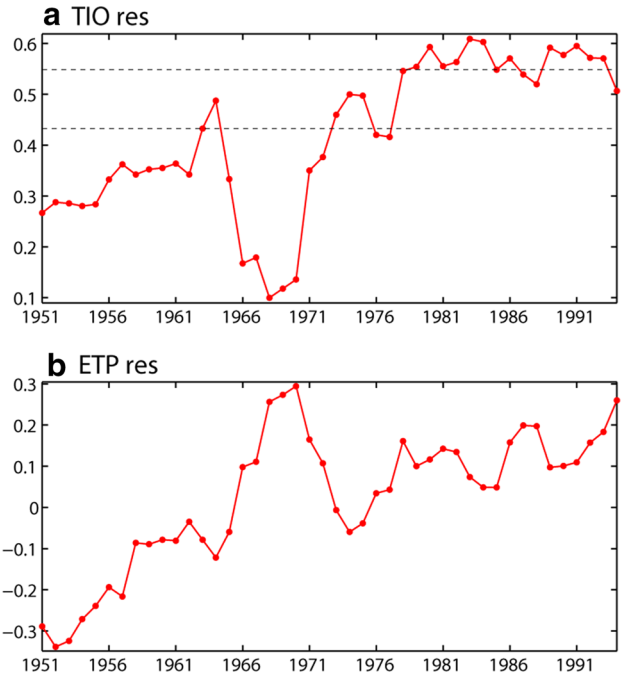

Fig. 10 The running partial correlations between the East Asian trough intensity index and **a** TIO index (ETP-free; referred to as TIO res) and **b** ETP index (TIO-free; referred to as ETP res) for the period 1951–2014, presented at the first year of a 21-year window. The dashed lines indicate the 95 and 99% confidence levels

Furthermore, during P2, the Maritime Continent convection activity (ETP-free) could generate a Rossby wave train-like meridional teleconnection pattern along the coast of North Pacific, imitating a WP pattern (Fig. 9). An anomalous anticyclone is observed over the East Asian coast region, which indicates a weakened East Asian trough. This distribution of the anomalous atmospheric circulation over the North Pacific is similar to the distributions associated with the independent TIO, demonstrating that convection over the Maritime Continent acts as a bridge linking the TIO SST variability and ECP after the late 1970s.

In the foregoing analyses, the East Asia trough is identified to be the critical system affecting the spring ECP, which is consistent with previous studies (e.g., Zuo and Zhang 2012). An East Asian trough intensity index is defined as the averaged geopotential height at 500 hPa over the region (120°–145°E, 27.5°–40°N), similar to a previous study (Sun et al. 2016). After excluding the ETP signal, the 21-year running correlations between the East Asian trough intensity index and the TIO index show an increasing trend, and they are stably significant over the period after the late 1970s, which confirms the close relationship between ECP and independent TIO SST variability during P2 (Fig. 10a). In contrast, without the contribution of the TIO, the running correlation coefficients between the Niño3 index and East Asian trough intensity index are not significant during the period 1951–2014, consistent with the weak relationship between independent ETP and ECP during P2 (Fig. 10b).

The aforementioned results suggest that, after excluding the contribution of the TIO, ETP SSTAs play a limited role in the ECP variability during P2. However, a close connection between spring ECP and TIO SST variabilities is identified during P2, which is independent from the ETP SST variability. In particular, the spatial structures of anomalous circulations associated with tropical SST and TIO-related (ETP-free) SST share high similarity during P2, which indicates that the strengthened impact of tropical SST on the circulations over East Asia after the late 1970s could be attributed to the variability of TIO SST. Considering that the ENSO signal is strongest in winter, the ETP variability in winter and that in spring are further excluded from TIO-related SST using dualistic regression, and the relationship between ECP and TIO SST is still significant after the late 1970s (figure not shown).

5 Model simulation

The analyses described in the previous sections indicate a close relationship between the spring ECP and TIO SST (ETP-free) after the late 1970s based on partial correlation and regression. Because the ETP signal could not be completely removed using observation analyses, the results of the numerical simulations are used to further investigate the role of the positive SST anomalies over the TIO. The numerical experiments were introduced in Sect. 2. The spatial distribution of the TIO SSTA associated with the ECP is examined, after removing the ETP signal, which also shows a basin mode. Thus, in the numerical simulation, a uniform 0.5 °C SST anomaly is added over the TIO; the simulated results show the individual effect of the tropical Indian Ocean SST. In addition, the climatology for the SST used in the simulation is similar to that observed during the period 1981–2014 (figure not shown). Therefore, the simulated results can feasibly represent the effect of the TIO SSTA after the late 1970s.

The spatial distribution of the simulated precipitation is highly similar to that observed, as shown in Fig. 11a. Corresponding to a warmer-than-normal TIO SST, significantly positive precipitation anomalies occur over most of East China, except for some regions over the southern coast and northeastern China, with weak negative anomalies. The zonal dipole structure in 500 hPa Omega could also be reproduced in the model, with anomalous upward and downward motion over the TIO and Maritime Continent, confirming the co-variability of convections over the TIO and Maritime Continent, through the change in the Indian Ocean Walker circulation (Fig. 11b). Significant ascent motion is also observed over a large area of East China, demonstrating the close relationship between TIO SSTA and ECP. Figure 11c depicts the numerically simulated geopotential

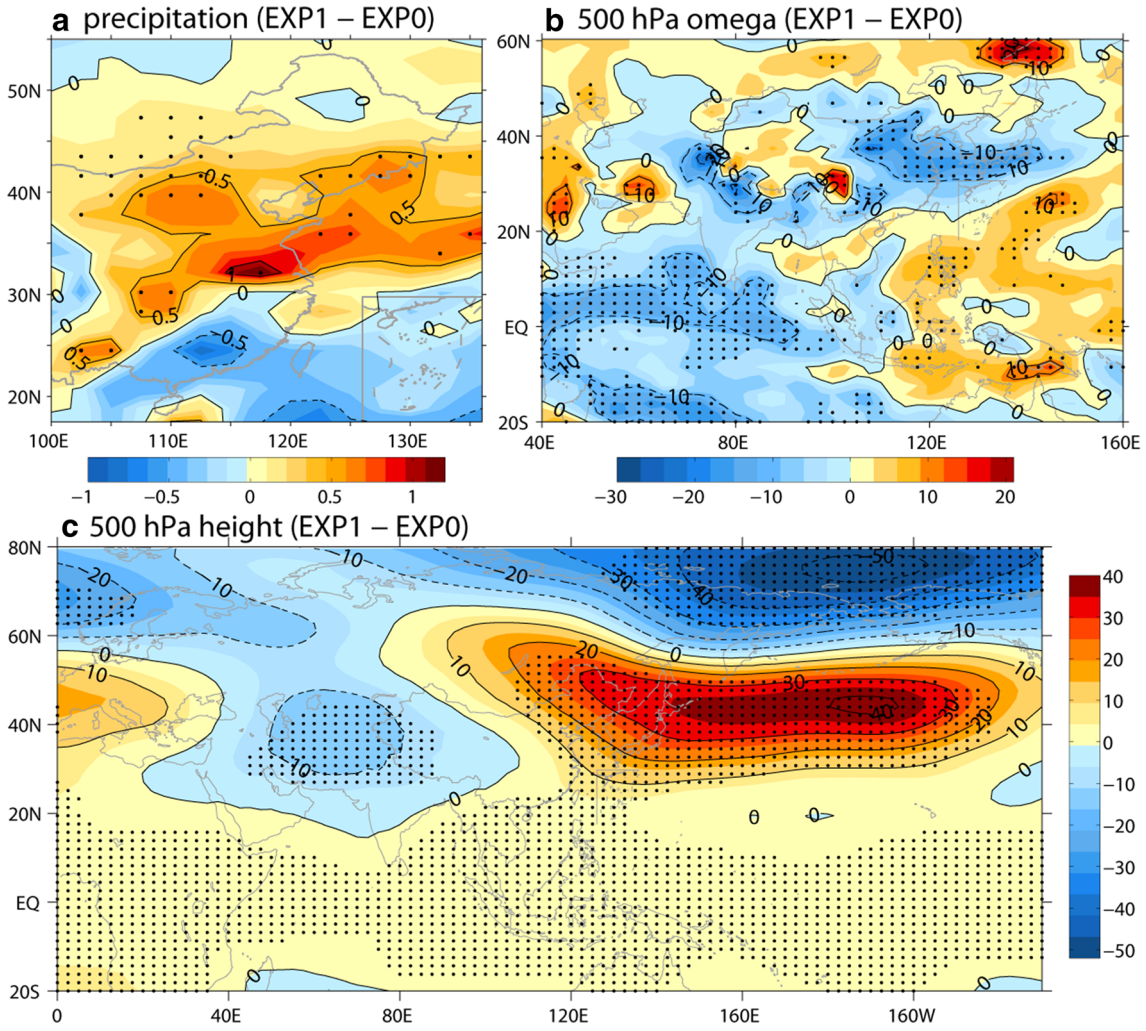

Fig. 11 Differences in **a** precipitation (mm day^{-1}), **b** 500 hPa omega (10^{-3} Pa s^{-1}) and **c** 500 hPa geopotential height (gpm) between the EXP1 and EXP0 in spring. Areas significant at the 95% confidence level are denoted by dots

heights at 500 hPa, whose spatial distribution resembles that obtained in the observation (Fig. 7e). Corresponding to a warmer TIO SST, significant zonally positive anomalies are observed to dominate the tropical region, between 20°S and 20°N. The significant WP pattern is also captured, with its positive center covering the East Asian region, suggesting a weakened East Asian trough. Additionally, over the mid-latitude Eurasian Continent, there is also a significant alternating anticyclone and cyclone teleconnection pattern, consistent with the observation. Note that the wave train-like pattern over the mid-latitude Eurasian Continent is not significant in the observation (Fig. 7e). Further investigation indicates that the atmospheric circulation variability over tropical North Atlantic could impact the Eurasian Continent mid-latitude circulation and further weaken the wave train-like pattern signal associated with the TIO warming. When the signal of tropical North Atlantic atmospheric circulation is removed using the linear regression method, the TIO SST-related atmospheric circulation shows a significant wave train-like pattern (figure not shown), similar to Fig. 11c. All signals are included in the observation data, therefore one systems' signal could be masked by another one in the observation analysis. In contrast, the atmosphere is forced only by the warming over TIO in the numerical simulation, which shows a significant wave pattern over mid-latitude Eurasian Continent. This result confirms that TIO warming could excite a Rossby wave train in the mid-latitude circulation over the Eurasian Continent, which contributes to the anomalous anticyclone over East Asia. The simulated atmospheric circulations and precipitation are highly consistent with observations associated with independent TIO, further confirming the connection between the TIO SST and ECP variability after the late 1970s.

6 Conclusions

The present study identified an enhanced response of spring precipitation over East China to the variability of tropical SST after the late 1970s. The dominant modes of ECP and tropical SST are highly correlated during the period after the late 1970s, consist with the interdecadal warming of tropical SST at the similar time. Furthermore, the two sub-periods 1951–1975 (P1) and 1981–2014 (P2) are selected for analysis. The SST PC1-related geopotential heights reveal notable differences over the mid-latitude North Pacific between the two sub-periods. During P1, NPO and PNA patterns are observed to dominate the North Pacific, which have a weak impact on the circulations over East Asia. In contrast, during P2, WP and PNA patterns are observed over the North Pacific. The significant positive anomalies of the WP pattern are observed to cover the East Asia region, indicating a weakened East Asian trough at 500 hPa. The southerlies along the western flank of the weakened East Asian trough favor the northward intrusion of warm and wet air into East China and enhance precipitation there. Additionally, the SST PC1-related anomalous Walker circulation is northwestward shifted and intensified after the late 1970s, consequently strengthening its impact on the ECP.

The tropical SST affecting the spring precipitation over East China has been investigated by some previous studies, and they mainly focused on the impact of ETP SST (e.g., Feng and Li 2011; Zuo et al. 2012; Wu and Mao 2016). This study shows that there is an enhanced influence of the tropical SST on the ECP after the late 1970s. In addition, through investigating the relative contributions of ETP and TIO SSTs to the variability of spring ECP during 1981–2014, we find that the SST variability over the ETP has a limited impact on ECP, while the SST over the TIO plays an essential role in the variability of ECP. For the climate prediction, the tropical pacific SST, in particular the ENSO situation, is generally emphasized. The result in this study indicates that, according to prediction of ECP in the boreal spring, the variability of SST over TIO should be mainly considered, which is more important than that over the ETP.

After the late 1970s, the physical progress of TIO SSTA affecting East Asian atmospheric circulation could be depicted as follow. The positive TIO SSTA could generate upward motion over the region and result in significant downward motion over the Maritime Continent through changing Indian Ocean Walker circulation. The suppressed convection activity over the Maritime Continent exerts further impacts on the East Asian atmospheric circulation, resulting in a weakened East Asian trough and enhanced convection over East China. In addition, the warmer-than-normal SST over the TIO could excite a zonal teleconnection pattern over the mid-latitude Eurasian Continent, which could also alter the status of the East Asian trough. The anomalous Rossby wave response along with the influence of the convection activity over the Maritime Continent modulate the spring precipitation over East China.

The observed physical processes associated with TIO SST are reproduced by the numerical simulations, providing further confirmation of the impact of the TIO SST variability on the spring ECP after the late 1970s. Because of the debatable accuracy of the decadal variability represented by the NCEP–NCAR reanalysis dataset, the analysis is also conducted using the Japanese 55-year reanalysis dataset (Ebita et al. 2011) and precipitation data from the Climate Research Unit (Harris et al. 2014). The results are consistent (figures not shown); thus, the findings of this study are robust.

Acknowledgements This work was jointly supported by the National Key Research and Development Program of China (Grant no. 2016YFA0600701), the National Natural Science Foundation of China (41421004 and 41522503), and the External Cooperation Program of BIC, Chinese Academy of Sciences (134111KYSB20150016).

References

Alexander MA, Blande I, Newman M et al (2002) The atmospheric bridge: the influence of ENSO teleconnections on air-sea interaction over the global oceans. J Clim 15:2205–2231

Annamalai H, Liu P, Xie SP (2005) Southwest Indian Ocean SST variability: its local effect and remote influence on Asian monsoon. J Clim 18:4150–4167

Chen J, Wen Z, Wu R, Chen Z, Zhao P (2014) Interdecadal changes in the relationship between southern China winter-spring precipitation and ENSO. Clim Dyn 43:1327–1338

Chen Z, Wen Z, Wu R, Lin X, Wang J (2015) Relative importance of tropical SST anomalies in maintaining the Western North Pacific anomalous anticyclone during El Niño to La Niña transition years. Clim Dyn 46:1027–1041

Ding Q, Wang B (2005) Circumglobal teleconnection in the Northern Hemisphere summer. J Clim 18:3483–3505

Ding RQ, Ha K-J, Li JP (2010) Interdecadal shift in the relationship between the East Asian summer monsoon and the tropical Indian Ocean. Clim Dyn 34:1059–1071

Ebita A, Kobayashi S, Ota Y et al (2011) The Japanese 55-year reanalysis "JRA-55": an interim report. Sola 7:149–152

Feng J, Li JP (2011) Influence of El Niño Modoki on spring rainfall over south China. J Geophys Res. https://doi.org/10.1029/2010JD015160

Fletcher CG, Cassou C (2015) The dynamical influence of separate teleconnections from the Pacific and Indian Oceans on the Northern Annular Mode. J Clim 28:7985–8002

Gent PR, Danabasoglu G, Donner LJ et al (2011) The community climate system model version 4. J Clim 24:4973–4991

Gill AE (1980) Some simple solutions for heat-induced tropical circulation. Quart J Roy Meteor Soc 106:447–462

Gong D, Ho C (2002) Shift in the summer rainfall over the Yangtze River Valley in the late 1970s. Geophys Res Lett. https://doi.org/10.1029/2001GL014523

Guo YJ, Yang XQ (2002) Temporal and spatial characteristics of interannual and interdecadal variations in the global ocean-atmosphere system (in Chinese). Sci Meteor Sin 22:127–138

Harris I, Jones PD, Osborn TJ, Lister DH (2014) Updated high-resolution grids of monthly climatic observations-the CRU TS3.10 dataset. Int J Climatol 34:623–642

Huang G, Hu K, Xie SP (2010) Strengthening of tropical Indian Ocean teleconnection to the Northwest Pacific since the mid-1970s: an atmospheric GCM study. J Clim 23:5294–5304

Huang BY, Banzon VF, Freeman E et al (2015) Extended reconstructed sea surface temperature version 4 (ERSST.v4). Part I: upgrades and intercomparisons. J Clim 28:911–930

Kalnay E, Kanamitsu M, Kistler R et al (1996) The NCEP/NCAR 40-year reanalysis project. Bull Am Meteorol Soc 77:437–471

Klein SA, Soden BJ, Lau N-C (1999) Remote sea surface temperature variations during ENSO: evidence for a tropical atmospheric bridge. J Clim 12:917–932

Kumar KK, Rajagopalan KB, Cane MA (1999) On the weakening relationship between the Indian monsoon and ENSO. Science 284:2156–2159

Lau N-C, Nath MJ (2003) Atmosphere–ocean variations in the Indo-Pacific sector during ENSO episodes. J Clim 16:3–20

Lau KM, Weng HY (1999) Interannual, decadal-interdecadal, and global warming signals in sea surface temperature during 1955–1997. J Clim 12:1257–1267

Li Y, Wu B, Yang Q, Huang S (2013) Different relationships between spring SST in the Indian and Pacific Oceans and summer precipitation in China. Act Meteor Sin 27:509–520

Li Z, Yang S, He B, Hu C (2016) Intensified springtime deep convection over the South China Sea and the Philippine sea dries Southern China. Sci Rep 6:30470. https://doi.org/10.1038/srep30470

Liu Z, Alexander MA (2007) Atmospheric bridge, oceanic tunnel, and global climatic teleconnections. Rev Geophys. https://doi.org/10.1029/2005RG000172

Nitta T, Yamada S (1989) Recent warming of tropical sea surface temperature and its relationship to the Northern Hemisphere circulation. J Meteorol Soc Japan 67:375–383

Qu X, Huang G (2012) An enhanced influence of tropical Indian Ocean on the South Asia High after the late 1970s. J Clim 25:6930–6941

Shao TH, Zhang YC (2012) Influence of winter North Atlantic Oscillation on spring precipitation in China. Plat Meteorol 31:1225–1233

Sun JQ (2012) Possible impact of the summer North Atlantic oscillation on extreme hot events in China. Atmos Oceanic Sci Lett 5:231–234

Sun JQ, Wang HJ (2012) Changes of the connection between the summer North Atlantic Oscillation and the East Asian summer rainfall. J Geophys Res. https://doi.org/10.1029/2012JD017482

Sun JQ, Wang HJ, Yuan W (2008) Decadal variations of the relationship between the summer North Atlantic Oscillation and middle East Asian air temperature. J Geophys Res. https://doi.org/10.1029/2007JD009626

Sun JQ, Wang HJ, Yuan W (2009) A possible mechanism for the covariability of the boreal spring Antarctic Oscillation and the Yangtze River valley summer rainfall. Int J of Climatol 29:1276–1284

Sun JQ, Wu S, Ao J (2016) Role of the North Pacific sea surface temperature in the East Asian winter monsoon decadal variability. Clim Dyn 46:3793–3805

Terray P, Dominiak S (2005) Indian Ocean sea surface temperatures and El Niño-southern oscillation: a new perspective. J Clim 18:1351–1368

Wang HJ (2002) The instability of the East Asian summer monsoon-ENSO relations. Adv Atmos Sci 19:1–11

Wang HJ, He SP (2012) Weakening relationship between East Asian winter monsoon and ENSO after mid-1970s. Chinese Sci Bull 57:3535–3540

Wang B, Wu R, Lau KM (2001) Interannual variability of the Asian summer monsoon: contrasts between the Indian and the western North Pacific-East Asian monsoons. J Clim 14:4073–4090

Wang HJ, Xue F, Zhou GQ (2002) The spring monsoon in South China and its relationship to large-scale circulation features. Adv Atmos Sci 19:651–664

Watanabe M, Jin FF (2003) A moist linear baroclinic model: coupled dynamical-convective response to El Niño. J Clim 16:1121–1139

Wu XF, Mao JY (2016) Interdecadal modulation of ENSO-related spring rainfall over South China by the Pacific Decadal Oscillation. Clim Dyn 47:3203–3220

Wu RG, Wang B (2002) A contrast of the East Asian summer Monsoon-ENSO relationship between 1962–77 and 1978–93. J Clim 15:3266–3279

Xie SP, Du Y, Huang G, Zheng XT, Tokinaga H, Hu KM, Liu QY (2010) Decadal shift in El Niño influences on Indo-Western Pacific and East Asian climate in the 1970s. J Clim 23:3352–3368

Xin X, Yu R, Zhou T, Wang B (2006) Drought in late spring of South China in recent decades. J Clim 19:3197–3206

Yim S-Y, Wang B, Liu J, Wu Z (2014) A comparison of regional monsoon variability using monsoon indices. Clim Dyn 43:1423–1437

Zhang J, Zhou T, Yu R, Xin X (2009) Atmospheric water vapor transport and corresponding typical anomalous spring rainfall patterns in China (in Chinese). Chin J Atmos Sci 33:121–134

Zhou BT (2011) Linkage between winter sea surface temperature east of Australia and summer precipitation in the Yangtze River valley and a possible physical mechanism. Chin Sci Bull 56:1821–1827

Zhou BT (2013) Weakening of winter North Atlantic Oscillation signal in spring precipitation over southern China. Atmos Ocean Sci Lett 6:248–252

Zhou BT, Wang HJ (2006) Relationship between the boreal spring Hadley circulation and the summer precipitation in the Yangtze River valley. J Geophys Res. https://doi.org/10.1029/2005JD007006

Zhou BT, Xia DD (2012) Interdecadal change of the connection between winter North Pacific Oscillation and summer precipitation in the Huaihe River valley. Sci China Earth Sci 55:2049–2057

Zhou BT, Zhao P (2010) Influence of the Asian-Pacific oscillation on spring precipitation over central eastern China. Adv Atmos Sci 27:575–582

Zhu YM, Yang XQ, Chen XY, Zhao SS, Sun XG (2007) Interdecadal variation of the relationship between ENSO and summer interannual climate variability in china (In Chinese). J Trop Meteorol 23:105–116

Zuo Z, Zhang R (2012) The anomalies of spring rainfall in eastern China and its relation with tropical Pacific SST and Eurasian snow (in Chinese). Chin J Atmos Sci 36:185–194